Editors' Suggestion | Featured in Physics

Relativistic Feedback Discharges in Dielectric Solids

Victor P. Pasko[1,*] Sebastien Celestin[2] and Anne Bourdon[3]

[1]School of Electrical Engineering and Computer Science, Penn State University, University Park, Pennsylvania 16802, USA
[2]Laboratory of Physics and Chemistry of the Environment and Space (LPC2E), OSUC, University of Orleans, CNRS, Orleans, France
[3]Laboratory of Plasma Physics (LPP), CNRS, Sorbonne Université, École Polytechnique, Institut Polytechnique de Paris, Palaiseau, France

(Received 6 November 2025; accepted 15 January 2026; published 5 March 2026)

The photoelectric feedback processes leading to growth of relativistic runaway electron avalanches are believed to be responsible for extreme fluxes of γ rays produced from very compact regions of space with dimensions on the order of a hundred meters in association with lightning activity in the Earth's natural environment [V. P. Pasko *et al.*, Photoelectric effect in air explains lightning initiation and terrestrial γ ray flashes, J. Geophys. Res. **130**, e2025JD043897 (2025)]. Here, we demonstrate for the first time that the same photoelectric feedback discharges can be realized on centimeter scales in common solid state dielectric materials, like quartz, acrylic, and bismuth germanate. These discharges can serve as new sources of high energy x-ray radiation.

DOI: 10.1103/4p6l-rzck

The maximum voltages achievable in lightning-related laboratory studies of meter long sparks in ambient air do not exceed 5–6 MV [1–7], and extensive list of references therein. Dwyer [8] discovered that in order to explain observed intensities of bursts of several tens of mega-electron-volt energies photons observed in Earth's atmosphere in association with lightning activity, and referred to as terrestrial γ ray flashes (TGFs) [9], a feedback mechanism should be involved in these events when an avalanche of relativistic electrons launches positrons and x-rays backward at its origin to provide additional seeding and replenishment of the avalanche. In order to achieve the observed energetics with ~7.3 MeV characteristic cutoff energy for both relativistic electrons and photons [10–12], and references therein, potential differences U on the order of 100 MV are required and are achievable in natural thundercloud environment [13]. For intuitive order of magnitude estimates, one can interpret eU, where e is the elementary electron charge, as an energy ε_e an electron can gain in a typical thundercloud with a charge $Q \sim 10$ C with a dimension $L \sim 1$ km in the air medium with relative permittivity $\epsilon_r \sim 1$, i.e., $\varepsilon_e \sim (1/4\pi\epsilon_r\epsilon_o)(Q/L) \sim 100$ MeV [Fig. 1(a)]. The gaps with 100 MV potential differences were employed in recent modeling that suggested that the photoelectric feedback plays the dominant role in production of TGFs and lightning initiation [14]. The available laboratory voltages cited above are clearly not sufficient for accurate studies of this phenomenology. Challenges of observing relativistic feedback discharges under laboratory conditions have been discussed in [15].

Sturge *et al.* [16,17] have recently suggested that polymethyl methacrylate (PMMA, $C_5H_8O_2$, also commonly referred to as acrylic) dielectric material with density $\rho_{PMMA} = 1.2\ \mathrm{g\,cm^{-3}}$ and relative permittivity $\epsilon_r \simeq 3$ [18], p. $V/87$ can accumulate significant charge densities when irradiated by a ~5 MeV electron beam leading to an electrical breakdown phenomenon that is analogical to that observed in lightning. We note that density of PMMA is approximately 1000 times that of ambient air $\rho_{air} = 1.2\ \mathrm{mg\,cm^{-3}}$ at ground pressure. The charge $Q \sim 734$ μC in PMMA can be produced by electron beam current of 5 mA applied over 0.15 s (consistent with the range of currents 3–9 mA and charging times 3–100 s experimentally explored in [16,17]). In PMMA the role of characteristic length L is played by an effective stopping distance

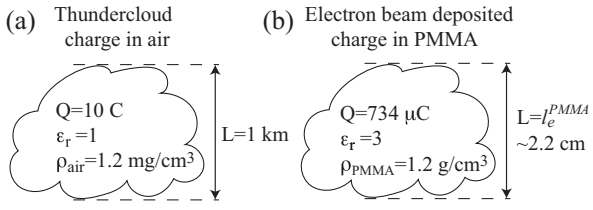

FIG. 1. (a) Schematic representation of a typical thundercloud charge Q and spatial scale L. To simplify discussion in this Letter we refer to air mass density ρ_{air} taken at sea, near ground level. (b) Similar scales defined for PMMA dielectric material recently studied in [16,17]. The parameters shown for both cases lead to identical 100 MV potential differences available for electron acceleration (see text for details).

*Contact author: vpasko@psu.edu

of 5 MeV electrons, $l_e^{\mathrm{PMMA}} \simeq 2.2$ cm [19] leading to a possibility to achieve very high $\varepsilon_e \sim (1/4\pi\epsilon_r\epsilon_o)(Q/L) \sim$ 100 MeV [Fig. 1(b)].

The goal of this Letter is to define conditions for relativistic feedback discharges on centimeter scales in solid dielectric materials. The quantitative results are reported for PMMA or acrylic, silicon dioxide or quartz (QTZ, SiO_2), and also in a representative high atomic number bismuth germanate dielectric material (BGO, $Bi_4Ge_3O_{12}$).

The principal modeling steps employed in the present Letter are the same as documented in [20]. The relativistic runaway electrons avalanche in one dimensional simulation domain with avalanche multiplication length l_r under application of constant electric field E_a and emit the bremsstrahlung x-rays due to their interactions with background material. The x-rays are attenuated due to the photoelectric absorption, Compton scattering, and pair production. The secondary relativistic runaway electrons are produced due to photoelectric absorption of x-rays in the volume of background material. Under the self-sustained steady state conditions, this photoelectric feedback process produces just enough secondary runaway electrons upstream of the avalanche to replicate itself. Only backward propagating bremsstrahlung photons seeding runaway electrons at the start of the avalanche make significant contribution to this process [14,20]. We note that this phenomenology is analogical to conventional positive corona discharges in air, where electron seeds are generated by photoionization far away from the maximum of electron density near coronating electrode [21]. The output of modeling is the corresponding threshold electric field E_0 for the photoelectric feedback discharge versus extent of space over which it is applied d (referred to as gap size in gaseous air medium studies reported in [20]).

Figure 2 shows dynamic friction force (stopping power in units of eV m^{-1}) acting on electrons in three studied materials as a function of electron energy ε_e. The maximum values are referred to as thermal runaway threshold fields E_c [22]. We associate the minimum fields in these curves, E_t, with an electric field required for development of relativistic runaway electron avalanche [23]. If electrons possess significant energy above ~0.1–1 keV corresponding to the E_c peaks, they can continue to gain energy (runaway) in relatively low applied fields $E_t < E_a < E_c$. It had been discovered by Gurevich *et al.* [23] that a fraction of secondary electrons produced by these runaways also can become runaways themselves leading to an avalanche multiplication of these electrons. The quantitative studies of this process are not yet available for studied materials at the same level of detail as in air [8,12,24], and in the present Letter we use minima in the dynamic friction force shown in Fig. 2 to approximate the related threshold E_t values. These fields are proportional to the product of molecular number density N_m and an average molecular nuclear

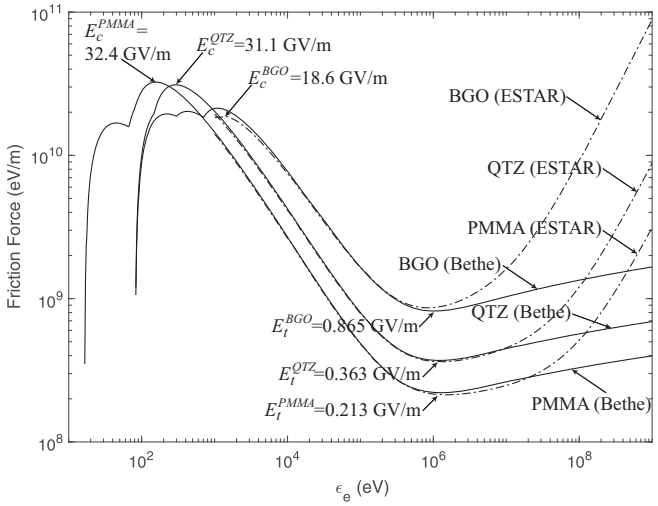

FIG. 2. Dynamic friction force on electrons in three studied materials: PMMA, QTZ, and BGO. The data represented by dash-dotted lines are from [19]. These distributions include electron radiation losses that become significant at energies above ~1 MeV. Solid lines are analytical representations using classic Bethe theory [29]. The peaks in these curves are referred to as thermal runaway threshold fields [22], and the figure includes related E_c numerical values adopted in the present Letter for the three studied materials. The fields corresponding to minimum in these curves around ~1 MeV are fields required for development of relativistic runaway electron avalanches E_t [23]. The figure includes related numerical values adopted for the three studied materials (see further discussion in the text).

charge Z_m, and the relative numerical differences between these fields values shown in Fig. 2 can be directly associated with related N_m values: 7.229×10^{21}cm^{-3}, 2.33×10^{22} cm^{-3}, and 3.447×10^{21} cm^{-3}, and Z_m values: 54, 30, and 524, for PMMA, QTZ, and BGO, respectively. Similarly to E_t the characteristic timescale $\tau = (2\pi N_m Z_m r_o^2 c)^{-1}$ and spatial scale τc of avalanche multiplication of relativistic runaway electrons directly depend on the product of N_m and Z_m. These scales are inversely proportional to $N_m Z_m$. Here, $c = 2.998 \times 10^8$ m s^{-1} is the speed of light in free space and $r_o = 2.818 \times 10^{-15}$ m is the classical electron radius. For air $Z_m = 14.5$ and at sea level air density $N_m = 2.688 \times 10^{25}$ m^{-3} these quantities can be estimated as $\tau = 172$ ns and $\tau c = 51$ m consistent with [25], p. 21, and [26]. The τc lengths are 5.13, 2.87, and 1.1 cm for PMMA, QTZ, and BGO, respectively, emphasizing the possibility of multiplication of relativistic runaway electrons on centimeter scales in these materials. The runaway electron energy distributions in PMMA, QTZ, and BGO have not yet been established. Because of a similar structure of the dynamic friction force as a function of energy for air [Fig. 2(a) in [20]] and PMMA, QTZ and BGO materials (Fig. 2) in this Letter we assume the normalized to unity energy distribution function $f_e(\varepsilon) = (1/\mathcal{E}_0)e^{-(\varepsilon/\mathcal{E}_0)}$ ($\mathcal{E}_0 = 7.3 \times 10^6$ eV) that was previously

used for relativistic runaway phenomena in air [12], and references therein. We note that to the order of magnitude $\mathcal{E}_0 \simeq E_t \tau c$ [27], Sec. 4.1.1, and $E_t \tau \simeq 21.7 mc/e$ [28], where m is electron rest mass. The product $E_t \tau$ does not depend on material specific product $Z_m N_m$. This is an additional consideration that strengthens the above common energy distribution assumption. Similarly to air [12], and references therein, the avalanche multiplication length l_r for PMMA, QTZ, and BGO is assumed to be controlled by the corresponding E_t thresholds for these materials shown in Fig. 2 and the applied electric field E_a. It is expressed as $l_r = [(\mathcal{E}_0/E_a)/(1 - E_t/E_a)]$.

The x-ray generation by runaway electrons in studied materials is characterized by doubly differential cross section of the bremsstrahlung photon production $(d^2\sigma_{br}/d\varepsilon_\gamma d\Omega)$, where the angular dependence is the one for the emitted photon [30], p. 245; [25], p. 45, and references therein. The bremsstrahlung photon production scales quadratically with atomic numbers of atoms constituting molecules in studied materials. The x-ray emission frequency per unit energy per one runaway electron [$eV^{-1}\ s^{-1}$] in BGO ($Bi_4Ge_3O_{12}$) material, for example, is

$$\nu_\gamma(\varepsilon_\gamma) = 19 N_m \int_{\varepsilon_\gamma}^{\infty} f_e(\varepsilon) \frac{d\sigma_{br}}{d\varepsilon_\gamma}(\varepsilon, \varepsilon_\gamma) v(\varepsilon) d\varepsilon, \qquad (1)$$

where factor 19 is the number of atoms in the BGO molecule, $v(\varepsilon) = c\sqrt{1 - [1 + \varepsilon/(mc^2)]^{-2}}$, and $(d\sigma_{br}/d\varepsilon_\gamma) = \int_\Omega (d^2\sigma_{br}/d\varepsilon_\gamma d\Omega) d\Omega$. For BGO the differential cross section $(d\sigma_{br}/d\varepsilon_\gamma)$ can be further expressed as a sum of atomic contributions from bismuth ($Z_{Bi} = 83$), germanium ($Z_{Ge} = 32$), and oxygen ($Z_O = 8$) atoms constituting the BGO molecule: $(d\sigma_{br}/d\varepsilon_\gamma) = (4/19)(d\sigma_{br}^{Bi}/d\varepsilon_\gamma) + (3/19)(d\sigma_{br}^{Ge}/d\varepsilon_\gamma) + (12/19)(d\sigma_{br}^{O}/d\varepsilon_\gamma)$. The total emission frequency of bremsstrahlung photons per one runaway electron [s^{-1}] is $\nu_\gamma^t = \int \nu_\gamma(\varepsilon_\gamma) d\varepsilon_\gamma$. The related values are $\nu_\gamma^t = 1.41 \times 10^{10}\ s^{-1}$, $4.33 \times 10^{10}\ s^{-1}$, and $5.78 \times 10^{11}\ s^{-1}$, for PMMA, QTZ, and BGO, respectively. We note that the number of x-ray photons is significantly higher in high-Z BGO material, however, electrons in this material also experience a stronger friction force (Fig. 2) leading to stronger electric field requirements in order to satisfy the photoelectric feedback discharge conditions. As will be discussed below the resultant threshold fields E_0 appear to be similar for all three materials studied in the present Letter.

The algorithms used in the calculation of the number of runaway electrons produced per unit volume per second due to photoelectric effect in the studied materials due to x-rays are the same as described in [20]. The formulation accounts for the volumetric emission source of photons, geometrical spreading and attenuation of photons as they propagate, and their absorption by target molecules constituting studied materials. The total absorption coefficients include the photoelectric absorption, Compton scattering, and pair production. Figure 3(a) illustrates the characteristic absorption lengths of photoelectric absorption l_{pe}, Compton scattering l_c, and pair production l_{pp} for three studied materials. We note that the values for l_{pp} for PMMA and QTZ are not shown as they appear outside of the upper bound of the vertical scale in Fig. 3(a). The photoelectric effect is strongest (has the shortest absorption length) for high-Z BGO material, as expected. On centimeter scales the photoelectric effect dominates Compton scattering and pair production for all three materials. For comparison, Fig. 3(a) also shows the electron range l_e for three studied materials over the same energy range. The vertical dashed

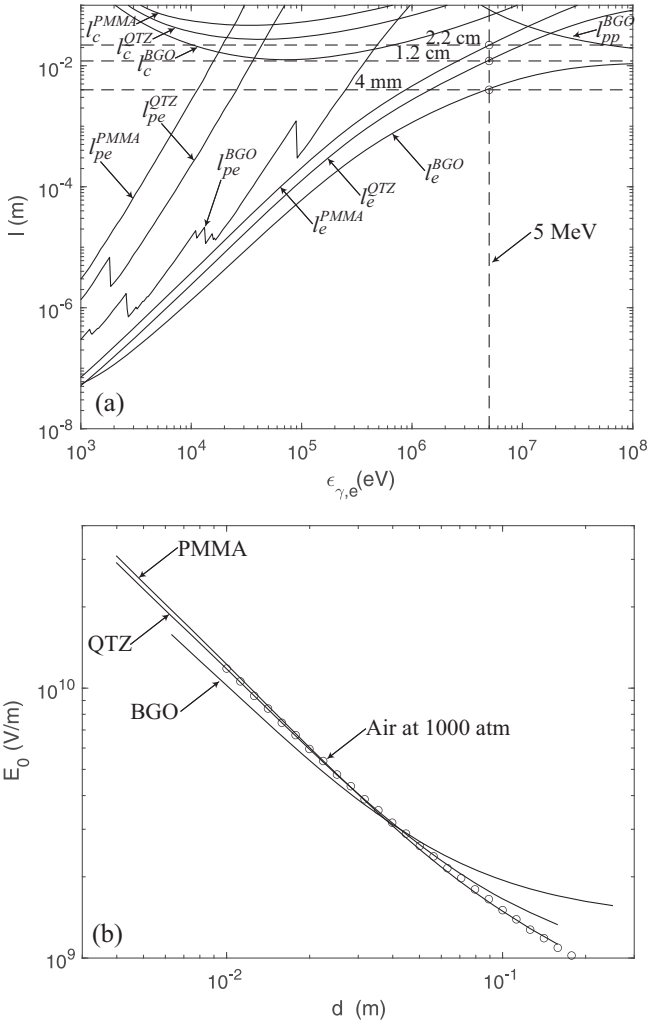

FIG. 3. (a) Attenuation lengths of photons (due to photoelectric absorption l_{pe}, Compton scattering l_c, and pair production l_{pp}), and electrons (l_e), in PMMA, QTZ, and BGO materials. The photon data are taken from [31]. The electron data are from [19] (see further discussion in the text); (b) the threshold electric field E_0 required for inception of relativistic runaway discharges as a function of length d over which this field is applied in studied materials. The open circles show results for air [14,20] at 1000 atm pressure.

line illustrates electron range values for 5 MeV electron beam energy used in [16,17]. These values are 2.2 cm [as already illustrated in Fig. 1(b)], 1.2 cm and 4 mm for PMMA, QTZ, and BGO, respectively.

Figure 3(b) reports the threshold electric field E_0 required for the inception of relativistic runaway discharges as a function of length d over which this field in applied in PMMA, QTZ, and BGO. As noted above, the PMMA mass density is approximately 1000 times that of air at ground pressure, and Fig. 3(b) also includes scaled results for air from [14,20] assuming 1000 atm air pressure. It is remarkable that the threshold fields appear to be similar for all these cases. Figure 3(b) suggests that relativistic feedback discharges can develop in studied materials on 1–10 cm spatial scales.

The available time dependent results for these discharges in air [14] indicate an extreme sensitivity to applied electric fields E_a above the E_0 threshold, when only several percent variations in E_a lead to orders of magnitude variations in γ ray production. For a near ground source in the Earth's atmosphere the total number of γ ray photons $N_\gamma \sim 3 \times 10^{16}$ is a good reference value for terrestrial γ ray flashes detected from the orbit that corresponds to 1 photon per cm^2 detector area at nominal 500 km satellite distance [32]. The quantitative analysis in [14] indicates that these discharges can produce orders of magnitude lower values of N_γ than 3×10^{16}, that are still easily detectable at close range. Such weak terrestrial γ ray flashes have been observed from high altitude aircraft [33] and from the ground [34–36]. The N_γ source values and durations of these discharges scale inversely proportionally with medium mass density [14]. The $N_\gamma \sim 3 \times 10^{16}$ and $\sim$1 μs typical discharge rise time at 1 atm, for example, lead to estimates of $N_\gamma \sim 3 \times 10^{13}$ and $\sim$1 ns rise time at 1000 atm. In comparison with the geophysical situation even 3 to 5 orders of magnitude weaker sources than 3×10^{13} still would lead to thousands of photons per cm^2 detector area positioned at $\sim$1 m from the source. In the present Letter, we do not quantify absorption and escape of these photons from studied materials. Attenuation lengths of photons shown in Fig. 3(a) indicate that the absorption is energy dependent. Additionally, any enclosure of the dielectric medium inside of shielding cavities formed by high Z materials (i.e., tungsten with $Z_W = 74$, or lead with $Z_{Pb} = 82$) should enhance backscattering of photons and support growth of relativistic feedback discharges. The quantitative predictions related to detectability of photons with different energies and the role of high Z shielding enclosures require further investigation.

The radiation losses represent only a small fraction of total energy losses in this system, that are dominated by electron collisions (Fig. 2). Our estimates indicate that average energy of x-ray photons for all three studied materials is approximately 360 keV, and only $\sim$0.05% (or 1.72 J) of total energy of 3.7 kJ supplied by the 5 MeV electron beam with parameters discussed with relation to Fig. 1(b) is converted to and emitted in the form of x-rays.

The total potential differences available for electron acceleration in considered model cases can be directly inferred from the product of E_0 and d in Fig. 3(b) and are on the order of 100 MV. The exact conditions for these discharges still require further investigation as similarly to large scale air discharges in thunderclouds these discharges are expected to be produced in the same physical space where streamer and leader discharges are produced as well [14]. Although it is expected that, similarly to air, the conventional breakdown field E_k for these discharges should reside between E_t and E_c, i.e., $E_t < E_k < E_c$, the accurate information about E_k under conditions of electron beam charging reported in [16,17] is not available. In air, streamer discharges can develop in fields below E_k if seeded by relatively high density regions of free electrons or by sharp electrodes. Sturge *et al.* [16], and references therein, notes that PMMA can withstand high electric fields between 0.3 to 0.6×10^9 V m^{-1} before it undergoes breakdown. For reference, the scaled value of E_k for air in Fig. 3(b) is $E_k \simeq 3.185 \times 10^9$ V m^{-1}.

In large volumes of air in the geophysical environment in Earth's atmosphere the seeding of photoelectric feedback discharges by electrons with $\sim$1 MeV energy is believed to be associated with a random arrival of cosmic rays [14], and discussion therein. In contrast, in [16,17] the 5 MeV electron beam provides an abundance of seed electrons.

X-rays from laboratory sparks have been observed under relatively low applied voltages [4–6,37–42], and are likely produced by cold runaway electrons produced due to streamers and/or leaders. The exact mechanisms of x-ray production in these discharges are not understood. The photoelectric feedback between cathode electrons and anode x-rays may be involved in the generation of a group of anomalously high energy electrons (up to three times applied voltage) observed experimentally [43], and references therein.

It has been suggested in [14] that in Earth's atmosphere (near 1 atm pressure air) photoelectric feedback discharges seed lightning and can be accompanied by exceptionally strong very high frequency (VHF, $\sim$100 MHz) radio noise due to streamer activity [44], and references therein. These naturally produced emissions are the strongest sources of terrestrial VHF radiation [44]. Having scaled up frequencies of these emissions by a factor of 1000 for studied materials (see discussion about frequency scaling in [45]), it is expected that photoelectric feedback initiated discharges in solid materials would produce strong extremely high frequency ($\sim$100 GHz) noise, analogical to VHF emissions at $\sim$1 atm in Earth's atmosphere. It is important to emphasize that discharges studied by Sturge *et al.* [16,17] were initiated by fast mechanical injection of a sharp tungsten electrode using a high pressure pneumatic

cylindrical system. This could be seen as analogous to triggering of lightning, and the discharge forms observed in [16,17] are likely related to streamers and leaders. The heating in leader channels is expected to be significantly accelerated in solid materials, as the related timescale is inversely proportional to the square of medium mass density [46,47].

In summary, this Letter creates new knowledge and provides quantitative predictions on the realization of electrical discharges driven by relativistic runaway electrons in solid state dielectric materials. These discharges develop on nanosecond time and centimeter spatial scales, and may potentially serve as new sources of high energy x-ray radiation and extremely high frequency radio emissions. As discussed in the text above, many questions remain that require further investigation: (a) the minimum electric field for these discharges; (b) the relativistic electron energy distribution; (c) the relativistic electron multiplication scale; (d) escape of x-rays from solid material and role of high Z enclosures; (e) the relation of these discharges to streamer and leader processes; and (f) the radio emissions from these discharges.

Acknowledgments—This research has been supported by the United States National Science Foundation under Grant No. AGS-2341623 to Penn State University. S. C. acknowledges support from the French space agency (CNES) within the projects OREO and STRATELEC, by the French Region Centre-Val-de-Loire, and by the Institut Universitaire de France (IUF).

Data availability—The data that support the findings of this article are openly available [19,31,48].

[1] M. Brook, G. Armstrong, R. Winder, C. Moore, and B. Vonnegut, Artificial initiation of lightning discharges, J. Geophys. Res. **66**, 3967 (1961).
[2] I. Gallimberti, G. Bacchiega, A. Bondiou-Clergerie, and P. Lalande, Fundamental processes in long air gap discharges, C. R. Phys. **3**, 1335 (2002).
[3] J. Dwyer, H. Rassoul, Z. Saleh, M. Uman, J. Jerauld, and J. Plumer, X-ray bursts produced by laboratory sparks in air, Geophys. Res. Lett. **32**, L20809 (2005).
[4] C. V. Nguyen, A. P. J. van Deursen, and U. Ebert, Multiple x-ray bursts from long discharges in air, J. Phys. D **41**, 234012 (2008).
[5] M. Rahman, V. Cooray, N. A. Ahmad, J. Nyberg, V. A. Rakov, and S. Sharma, X rays from 80-cm long sparks in air, Geophys. Res. Lett. **35**, L06805 (2008).
[6] P. O. Kochkin, A. P. J. van Deursen, and U. Ebert, Experimental study on hard x-rays emitted from metre-scale negative discharges in air, J. Phys. D **48**, 025205 (2015).
[7] A. Y. Kostinskiy, V. S. Syssoev, N. A. Bogatov, E. A. Mareev, M. G. Andreev, M. U. Bulatov, D. I. Sukharevsky, and V. A. Rakov, Abrupt elongation (stepping) of negative and positive leaders culminating in an intense corona streamer burst: Observations in long sparks and implications for lightning, J. Geophys. Res. **123**, 5360 (2018).
[8] J. R. Dwyer, A fundamental limit on electric fields in air, Geophys. Res. Lett. **30**, 2055 (2003).
[9] G. J. Fishman, P. N. Bhat, R. Mallozzi, J. M. Horack, T. Koshut, C. Kouveliotou, G. N. Pendleton, C. A. Meegan, R. B. Wilson, W. S. Paciesas, S. J. Goodman, and H. J. Christian, Discovery of intense gamma-ray flashes of atmospheric origin, Science **264**, 1313 (1994).
[10] D. M. Smith, L. I. Lopez, R. P. Lin, and C. P. Barrington-Leigh, Terrestrial gamma-ray flashes observed up to 20 MeV, Science **307**, 1085 (2005).
[11] W. Xu, S. Celestin, and V. P. Pasko, Source altitudes of terrestrial gamma-ray flashes produced by lightning leaders, Geophys. Res. Lett. **39**, L08801 (2012).
[12] J. R. Dwyer, D. M. Smith, and S. A. Cummer, High-energy atmospheric physics: Terrestrial gamma-ray flashes and related phenomena, Space Sci. Rev. **173**, 133 (2012).
[13] S. A. Mallios, S. Celestin, and V. P. Pasko, Production of very high potential differences by intracloud lightning discharges in connection with terrestrial γ ray flashes, J. Geophys. Res. **118**, 912 (2013).
[14] V. P. Pasko, S. Celestin, A. Bourdon, R. Janalizadeh, Z. Pervez, J. Jansky, and P. Gourbin, Photoelectric effect in air explains lightning initiation and terrestrial γ ray flashes, J. Geophys. Res. **130**, e2025JD043897 (2025).
[15] J. R. Dwyer, Relativistic breakdown in planetary atmospheres, Phys. Plasmas **14**, 042901 (2007).
[16] K. M. Sturge *et al.*, Dynamics of high-speed electrical tree growth in electron-irradiated polymethyl methacrylate, Science **385**, 300 (2024).
[17] K. M. Sturge, N. Hoppis, B. L. Beaudoin, A. M. Shearin, E. T. Basinger, B. C. Clifford, J. R. FitzGibbon, E. H. Frashure, J. E. Krutzler, A. A. Levitan, P. O'Shea, H. J. Wilson, and T. W. Koeth, Characterization of electrostatic discharge currents in electron-charged polymethyl methacrylate as a proxy for natural compact intracloud discharges, Phys. Rev. E **111**, 065207 (2025).
[18] *Polymer Handbook*, edited by J. Brandrup, E. H. Immergut, E. A. Grulke, A. Abe, and D. R. Bloch, 4th ed. (John Wiley & Sons, New York, 2005).
[19] National Institute of Standards and Technology, ESTAR: Stopping-power & range tables for electrons, https://physics.nist.gov/PhysRefData/Star/Text/ESTAR.html (accessed 6 November 2025).
[20] V. P. Pasko, S. Celestin, A. Bourdon, R. Janalizadeh, and J. Jansky, Conditions for inception of relativistic runaway discharges in air, Geophys. Res. Lett. **50**, e2022GL102710 (2023).
[21] G. V. Naidis, Conditions for inception of positive corona discharges in air, J. Phys. D **38**, 2211 (2005).
[22] A. V. Gurevich, On the theory of runaway electrons, Sov. Phys. JETP **12**, 904 (1961).
[23] A. V. Gurevich, G. M. Milikh, and R. A. Roussel-Dupré, Runaway electron mechanism of air breakdown and preconditioning during a thunderstorm, Phys. Lett. A **165**, 463 (1992).
[24] L. M. Coleman and J. R. Dwyer, Propagation speed of runaway electron avalanches, Geophys. Res. Lett. **33**, L11810 (2006).

[25] N. G. Lehtinen, Relativistic runaway electrons above thunderstorms, Ph.D. thesis, Stanford University, Stanford, CA, 2000.
[26] S. Celestin and V. P. Pasko, Soft collisions in relativistic runaway electron avalanches, J. Phys. D **43**, 315206 (2010).
[27] S. Celestin, W. Xu, and V. P. Pasko, Terrestrial γ ray flashes with energies up to 100 MeV produced by nonequilibrium acceleration of electrons in lightning, J. Geophys. Res. **117**, A05315 (2012).
[28] N. G. Lehtinen, T. F. Bell, and U. S. Inan, Monte Carlo simulation of runaway MeV electron breakdown with application to red sprites and terrestrial γ ray flashes, J. Geophys. Res. **104**, 24699 (1999).
[29] M. J. Berger and S. M. Seltzer, *Stopping Powers and Ranges of Electrons and Positrons (NBSIR 82-2550)* (U.S. Department of Commerce, Washington DC, 2005).
[30] W. Heitler, *The Quantum Theory of Radiation* 3rd ed. (Clarendon, Oxford, 1954).
[31] National Institute of Standards and Technology, XCOM: Photon cross sections database (http://www.nist.gov/pml/data/xcom), accessed November 6, 2025.
[32] B. E. Carlson, N. G. Lehtinen, and U. S. Inan, Neutron production in terrestrial γ ray flashes, J. Geophys. Res. **115**, A00E19 (2010).
[33] I. Bjorge-Engeland *et al.*, Evidence of a new population of weak terrestrial gamma-ray flashes observed from aircraft altitude, Geophys. Res. Lett. **51**, e2024GL110395 (2024).
[34] R. U. Abbasi *et al.*, Gamma ray showers observed at ground level in coincidence with downward lightning leaders, J. Geophys. Res. **123**, 6864 (2018).
[35] J. W. Belz *et al.*, Observations of the origin of downward terrestrial gamma-ray flashes, J. Geophys. Res. **125**, e2019JD031940 (2020).
[36] R. U. Abbasi *et al.*, Intermediate fluence downward terrestrial γ ray flashes as observed by the Telescope Array Surface Detector, J. Geophys. Res. **129**, e2024JD041260 (2024).
[37] Y. L. Stankevich and V. G. Kalinin, Fast electrons and x-ray radiation during the initial stage of growth of a pulsed spark discharge in air, Sov. Phys. Dokl. **12**, 1042 (1967).
[38] J. R. Dwyer, Z. Saleh, H. K. Rassoul, D. Concha, M. Rahman, V. Cooray, J. Jerauld, M. A. Uman, and V. A. Rakov, A study of x-ray emission from laboratory sparks in air at atmospheric pressure, J. Geophys. Res. **113**, D23207 (2008).
[39] C. L. da Silva, R. M. Millan, D. G. McGaw, C. T. Yu, A. S. Putter, J. LaBelle, and J. Dwyer, Laboratory measurements of x-ray emissions from centimeter-long streamer corona discharges, Geophys. Res. Lett. **44**, 11174 (2017).
[40] V. Tarasenko, Runaway electrons in diffuse gas discharges, Plasma Sources Sci. Technol. **29**, 034001 (2020).
[41] E. V. Parkevich, K. V. Shpakov, I. S. Baidin, A. A. Rodionov, A. I. Khirianova, T. F. Khirianov, Y. K. Bolotov, M. A. Medvedev, V. A. Ryabov, Y. K. Kurilenkov, and A. V. Oginov, Streamer formation processes trigger intense x-ray and high-frequency radio emissions in a high-voltage discharge, Phys. Rev. E **105**, L053201 (2022).
[42] L. Contreras-Vidal, C. L. da Silva, and R. G. Sonnenfeld, Production of runaway electrons and x-rays during streamer inception phase, J. Phys. D **56**, 055201 (2023).
[43] V. P. Pasko, S. Celestin, and A. Bourdon, Photoelectric feedback mechanism for acceleration of runaway electrons in gas discharges at high overvoltages, Phys. Rev. Lett. **133**, 235301 (2024).
[44] W. Rison, P. R. Krehbiel, M. G. Stock, H. E. Edens, X.-M. Shao, R. J. Thomas, M. A. Stanley, and Y. Zhang, Observations of narrow bipolar events reveal how lightning is initiated in thunderstorms, Nat. Commun. **7**, 10721 (2016).
[45] Z. Pervez, R. Janalizadeh, and V. P. Pasko, Measuring streamer producing thundercloud electric fields using radio observations of narrow bipolar events, Geophys. Res. Lett. **52**, e2025GL118469 (2025).
[46] J. A. Riousset, V. P. Pasko, and A. Bourdon, Air-density-dependent model for analysis of air heating associated with streamers, leaders, and transient luminous events, J. Geophys. Res. **115**, A12321 (2010).
[47] C. L. da Silva and V. P. Pasko, Dynamics of streamer-to-leader transition at reduced air densities and its implications for propagation of lightning leaders and gigantic jets, J. Geophys. Res. **118**, 13,561 (2013).
[48] V. P. Pasko, S. Celestin, and A. Bourdon, Relativistic feedback discharges in dielectric solids [Dataset], Penn State Data Commons, 10.26208/WS96-WN71 (2026).